X-RAY PULSARS

K.A. Postnov (Sternberg Astronomical Institute, Moscow)

Credits

- Co-authors:

  N. Shakura,
  A. Kochetkova,
  L.Hjalmarsdotter
  (SAI)

(MNRAS, submitted)

- Data provided by:

- V. Doroshenko, D. Klochkov (IAAT)
- A. Conzalez-Galan (U. Alicante)

Plan

- Recent highlights
- Disk and wind-fed pulsars
- Quasi-spherical accretion: new findings
- Conclusions

Introduction

- 1970, V. Shvartsman, accreting magnetized NS in binary systems
- 1971, UHURU discovery (Cen X-3, Giacconi et al.)
- 1976, First cyclotron line measurements (Her X-1, Truemper et al.)
- Later X-ray missions: spectra, pulse profiles, timing…

Cyclotron lines

272 R. Staubert (2003)

Table 1 Cyclotron Line Sources

System	Type	P_{spin} (s)	P_{orb} (days)	Ecl.	Line E. (keV)	Instr. of 1st Det.
RXTE:						
Hercules X-1	LMXB[a]	1.2377	1.70	yes	41	Balloon
4U 0115+63	Be trans.	3.61	24.3	yes	12	HEAO-1
Centaurus X-3	HMXB[b]	4.82	2.09	yes	28	BeppoSAX
4U 1626–67	LMXB	7.67	0.0289	no	37	BeppoSAX
XTE J1946+274	Transient	15.83	–	no	36	RXTE
Vela X-1	HMXB	283.2	8.96	yes	25	HEXE
4U 1907+09	HMXB	440.4	8.38	nearly	18	Ginga
4U 1538–52	HMXB	528.8	3.73	yes	20	Ginga
GX 301–2	HMXB	681	41.5	nearly	37	Ginga
4U 0352+309	Be persist.	837.7	250.3	no	29	RXTE
non-RXTE:						
A 0535+26	Be trans.	103	111	no	50, 110	HEXE/OSSE
V 0332+53	Be trans.	4.4	34	no	28	Ginga
Cep X-4	Be trans.	66.2	(100?)	no	30	Ginga

Variety of properties

- Persistent X-ray pulsars:
  - HMXBs:
    - wind-fed (Vela X-12, GX 301-2, GX 1+4…)
    - disk-fed (Cen X-3)
  - LMXBs:
    - disk-fed (Her X-1, 4U1626-67…)
    - Accreting millisecond XPSRs
- Transients: HMXBs, mostly young NS in eccentric orbits around Be-stars (A0535+26, V0332+53, 4U 0115+63…)

Spectral and timing properties

- Spectra and pulse shapes: accretion columns (radiation transfer in high magnetic field)
- Timing: interaction of NS magnetosphere with accreting matter
- Rich phenomenology (spectral-timing correlations, phase-resolved spectroscopy, …)

Disk-fed

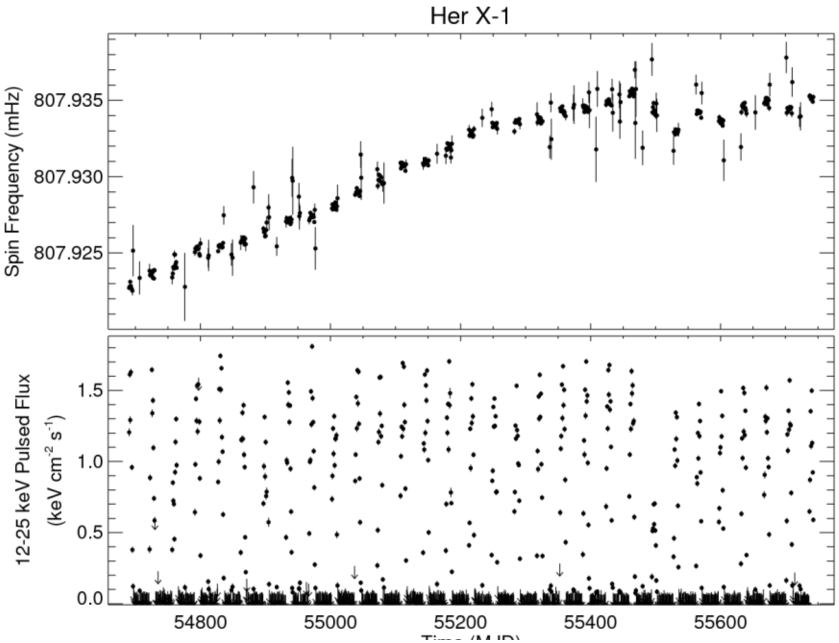

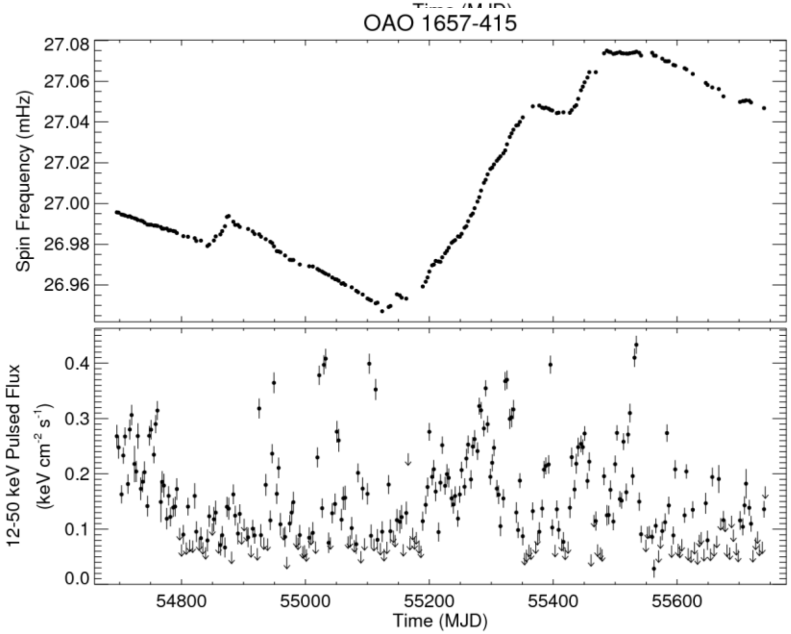

Wind-fed

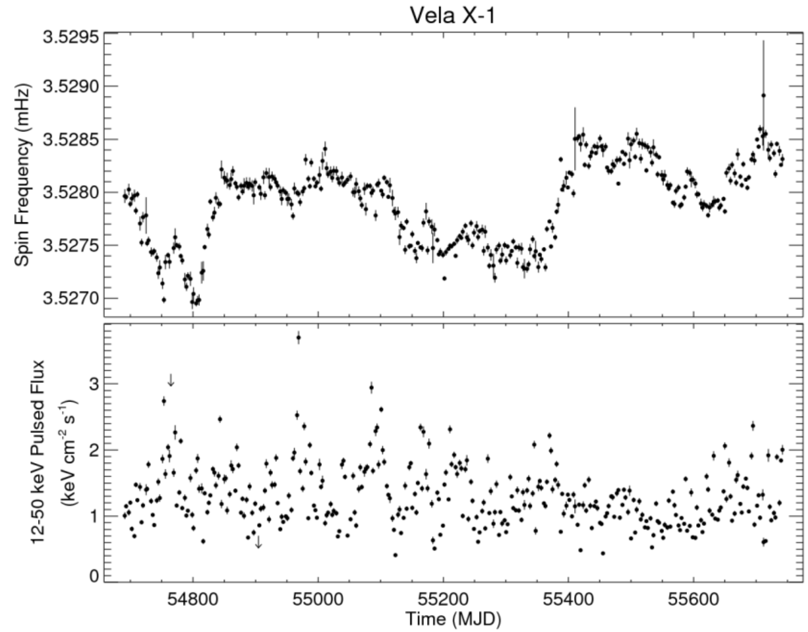

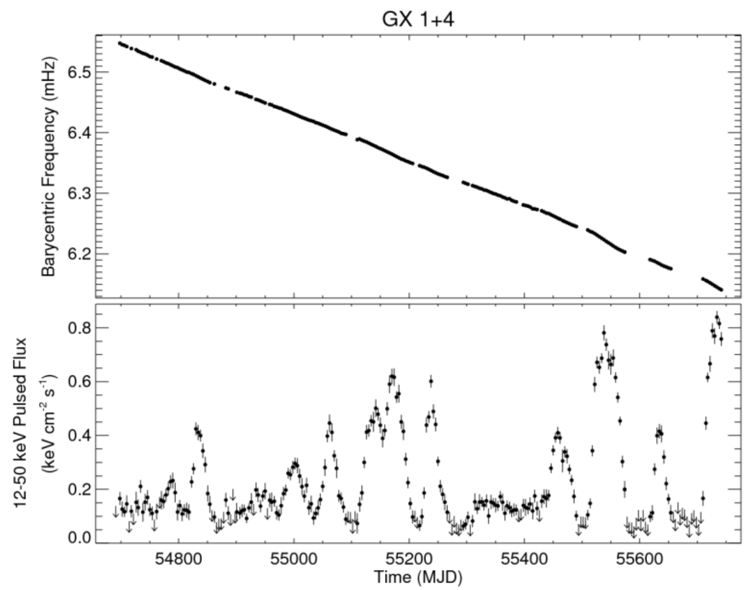

- Accretion columns:
  - Cyclotron line energy – X-ray luminosity correlations (different in high- and low-luminosity pulsars)
  - Pulse profile – X-ray luminosity/energy correlations

V0332+53

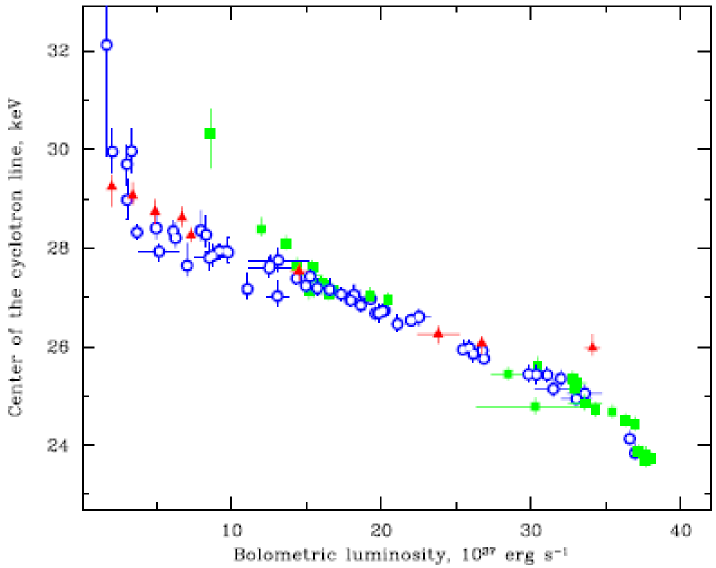

Her X-1 (also Vasco et al.2011)

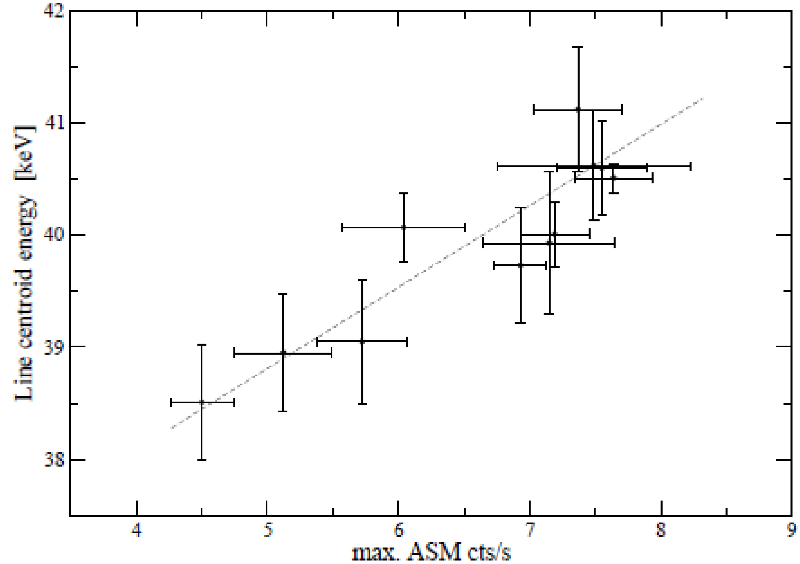

4U0115+63

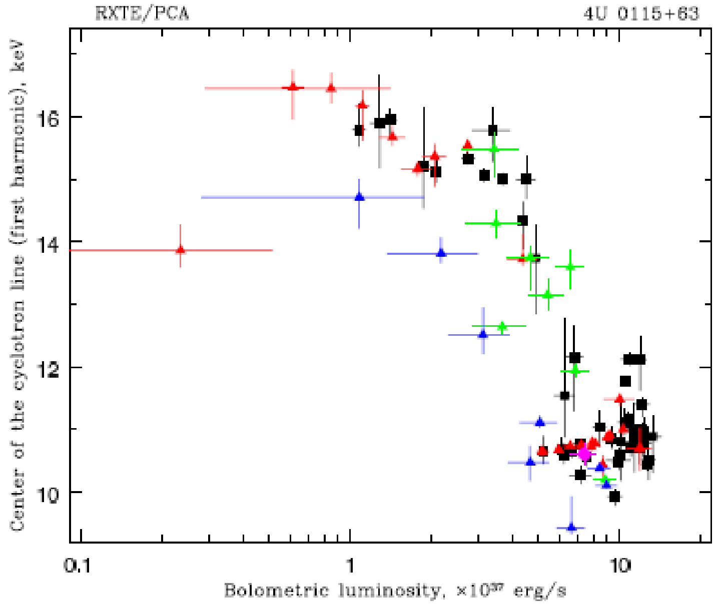

Figure 1: The different cyclotron line energy dependences on the X-ray flux as observed for V0332+53 (Tsygankov et. al., 2006; 2010), Her X-1 (Staubert et al., 2007),and 4U0115+63 (Tsygankov et. al., 2007).

This correlation is also seen in the pulse-to-pulse analysis:

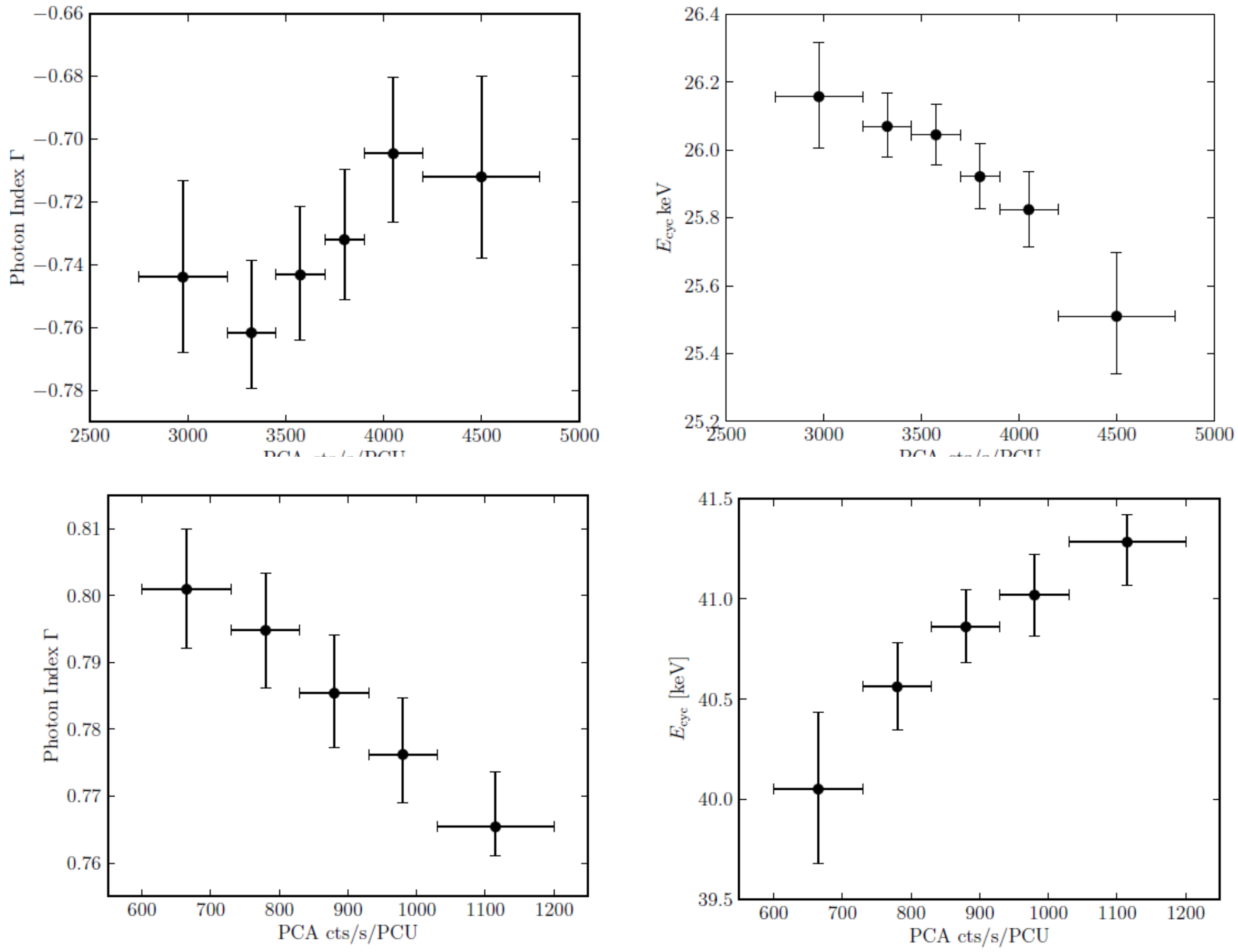

V0332

Her X-1

Klochkov et al. 2010

- **Magnetospheric interaction:**
  - Torque – X-ray luminosity correlations in disk-fed (Her X-1) and wind-fed (Vela X-1, GX 301-2, GX 1+4) pulsars (to be discussed later in more detail)

Her X-1, Klochkov et al. 2009

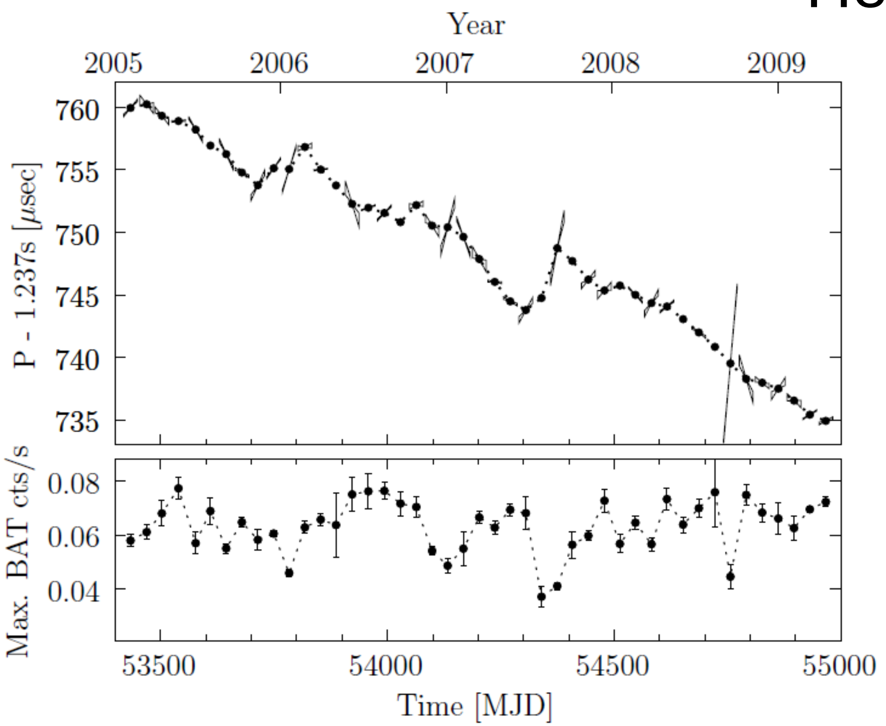

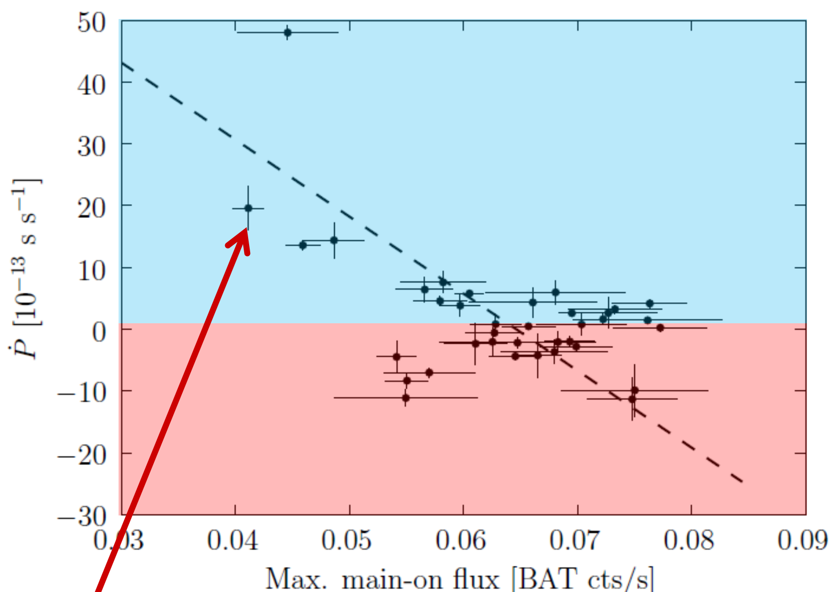

Mass ejection episodes

$$I\omega\dot{\omega} \sim \dot{M}_{\rm ej}\frac{GM}{R_c}$$

Key physical parameters

- NS magnetic field
  - Directly probed by CRSF energy (local - in the site of the line generation!)
  - Indirectly – from matter-magnetospheric interaction (only large-scale dipole component!)
- Mass accretion rate
  - Derived from X-ray luminosity, but the distance is usually uncertain

Alfven radius: definition in disk-accreting NS

$$\frac{R}{H}\frac{\mu^2}{2\pi R^6} = P(R) = \frac{\rho c_s^2}{\gamma}$$

$$\mu = \frac{1}{2}B_0 R_0^3$$

$$\dot{M} = 2\pi RH\rho v_R = 2\pi RH\rho\alpha c_s\left(\frac{H}{R}\right)$$

$$\boxed{R_A = \left[\frac{\alpha\gamma\mu^2}{\dot{M}\sqrt{GM}}\right]^{2/7}}$$

$$c_s = \left(\frac{H}{R}\right)v_\varphi = \left(\frac{H}{R}\right)\sqrt{\frac{GM}{R}}$$

Spin-up/spin-down equation

$$I\dot{\omega}^* = -A_d\frac{\mu^2}{R_c^3} + B_d\dot{M}\sqrt{GMR_A}$$

NS equilibrium period

$$P_{eq,d} \approx 7\mathrm{s}\left(\frac{A_d}{B_d}\right)^{1/2}\alpha^{-1/14}\mu_{30}^{6/7}\dot{M}_{16}^{-3/7}$$

Magnetospheric boundary

- Can be probed by X-ray timing analysis (noise power spectral shape)

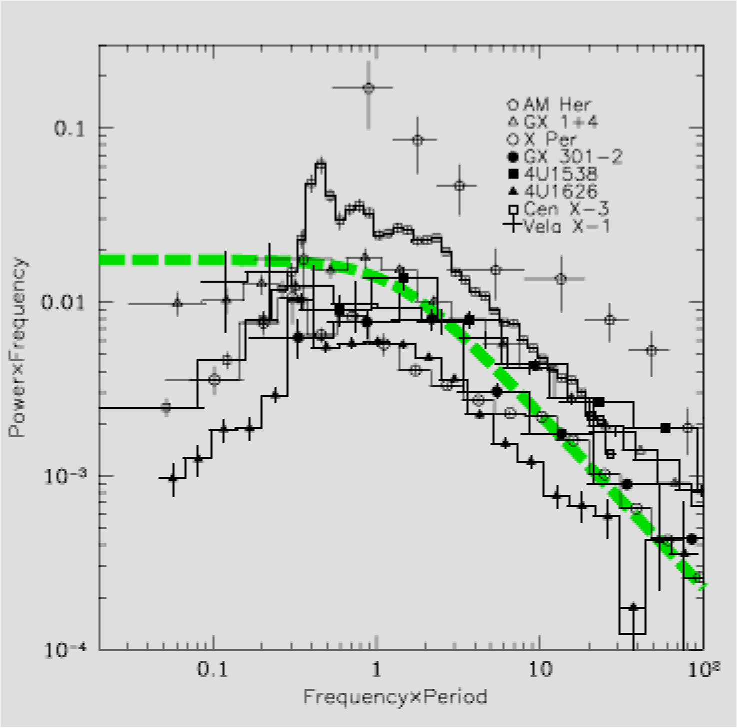

Revnivtsev et al. 2009

$$f_{\rm b} \propto L_{\rm x}{}^{3/7}$$

$$2\pi\nu_{\rm K} = (GM)^{1/2} R_{\rm m}^{-3/2}$$

$$R_{\rm m} \approx \mu^{4/7} (GM)^{-1/7} \dot{M}^{-2/7}$$

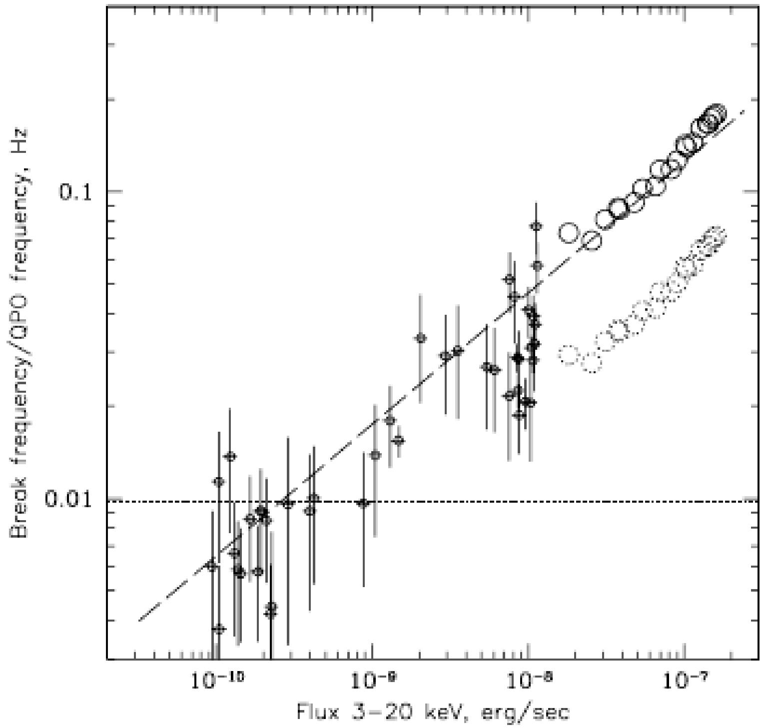

Frequency break dependence on X-ray luminosity reflects the dependence of Alfven radius on mass accretion rate

A0535+26 outburst

Alfven radius in wind-fed pulsars

- Two cases:
  - free-fall (Bondi) accretion (realized at large X-ray luminosities). Dynamical pressure at the magnetosphere
  - Subsonic (settling) accretion. More complicated: pressure due to temperature and other degrees of freedom (turbulence)

- In the case of free-fall accretion only spin-up of NS is possible (unless matter outflow from the NS magnetosphere is present, e.g. Illarionov & Kompaneets 1991)
- In the case of settling accretion, steady spin-down of NS is possible (the convective shell mediates the angular momentum transfer outward)

Subsonic settling accretion without shock near magnetosphere

Stellar wind from the secondary

Matter subsonically settles down inside the spherization radius R'_B

Convective isomomentum shell $\omega(R) \sim 1/R^2$

R_A - Alfven radius of NS

$R_B \sim 2GM/V^2$ (Bondi radius) characterizes bow shock location in the wind

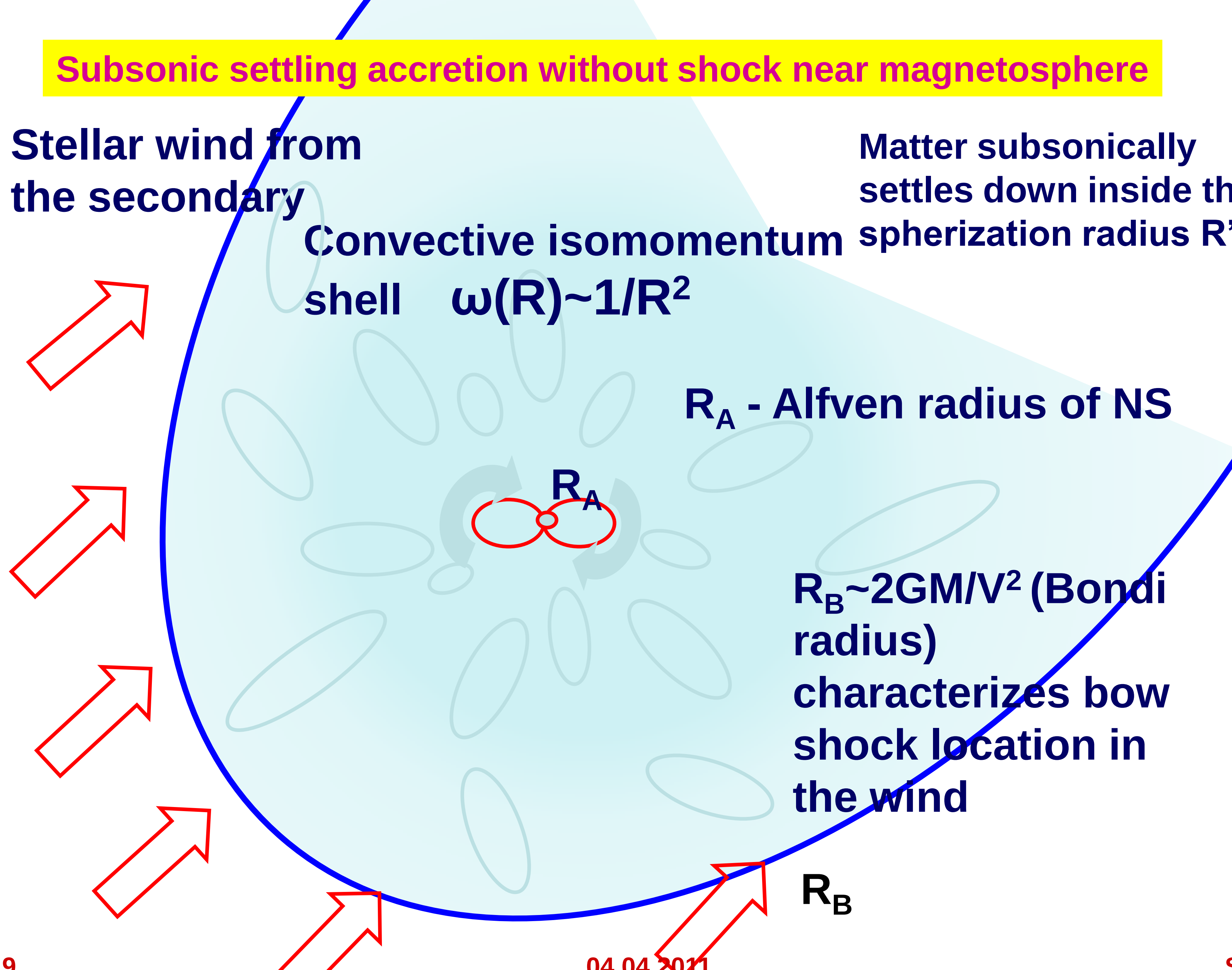

Settling accretion regime.
1.Alfven radius

$$K_2 \frac{\mu^2}{2\pi R^6} = P(R) = P_{gas} + P_{turb} + \ldots = \frac{\rho \mathbb{R} T}{\mu_m}(1 + P_{turb} / P_{gas} + \ldots)$$

$$\dot{M} = 4\pi\rho R^2 f(u)\sqrt{\frac{2GM}{R}}, \quad f(u) < 1$$

Thermal structure of the shell (hydrostatic equilibrium)

$$\frac{\mathcal{R}T}{\mu_m} = \frac{\gamma - 1}{\gamma}\frac{GM}{R}\left(\frac{1}{1 + \gamma m_\parallel^2 - 2(\gamma - 1)(m_\parallel^2 - m_\perp^2)}\right) = \frac{\gamma - 1}{\gamma}\frac{GM}{R} f(\gamma, m_t)$$

$m_\parallel^2$ and $m_\perp^2$ are turbulent Mach numbers squared in the radial and tangential directions.

$$R_A = \left[\frac{4\gamma}{(\gamma-1)}\frac{f(u)K_2}{f(\gamma,m_t)(1+\gamma m_t^2)}\frac{\mu^2}{\dot{M}\sqrt{2GM}}\right]^{2/7}$$

K_2~7.6 , f(u)~0.1
(Arons & Lea, 1976)
model

$$For \;\; \gamma = 5/3: \;\; \frac{4\gamma}{\gamma - 1} = 10$$

- Accretion rate in the settling accretion regime is determined by the ability of plasma to enter the NS magnetosphere (f(u))
- Appearance of dM/dt in the expression for Alfven radius is formal

2. Angular momentum transfer

- Plasma-magnetospheric interaction is characterized by the coupling constant K_1

$$B_t = K_1(\theta) B_p(\omega_m - \omega^*) t_{inst} \qquad t_{inst} = \frac{1}{\omega_K(R_A)}$$

Torque due to magnetic forces

$$I\dot{\omega}^* = \int \frac{B_t B_p}{4\pi} \varpi dS = -K_1(\theta) \frac{K_2}{(1+\gamma m_t^2)} \frac{\mu^2}{R_A^3} \frac{\omega^* - \omega_m}{\omega_K(R_A)}$$

Or in more familiar form: $I\dot{\omega}^* = Z\dot{M}R_A^2(\omega_m - \omega^*)$

Here the dimensionless coefficient Z is

$$Z = \frac{K_1(\theta)}{f(u)} \frac{\sqrt{2}(\gamma - 1)}{4\gamma} f(\gamma, m_t).$$

NB: ZdM/dt is independent of mass accretion rate!!!!

Total torque applied to NS:

$$\boxed{I\dot{\omega}^* = Z\dot{M}R_A^2(\omega_m - \omega^*) + z\dot{M}R_A^2\omega^*}$$

(Cf.: for free-fall accretion Z=z. By the angular momentum conservation

$$\omega_m = \omega_B(R_B/R_A)^2$$

$$I\dot{\omega}^* = Z\dot{M}\omega_B R_B^2 ,$$

where $Z \approx 1/4$ (Illarionov & Sunyaev 1975).

All we need to know is what is the angular velocity of matter near the magnetosphere. This depends on the angular momentum transfer through the convective shell. Solving gas-dynamic problem , we find:

$$\omega_m = \tilde{\omega}\omega_B\left(\frac{R_B}{R_A}\right)^n$$

Typically, n~2, but n=3/2 is also possible

INTERMEZZO: Gas-dynamics of settling accretion

1. Mass continuity equation:

$$\frac{\partial \rho}{\partial t} + \frac{1}{R^2}\frac{\partial}{\partial R}\left(R^2 \rho u_R\right) + \frac{1}{R\sin\theta}\frac{\partial}{\partial\theta}(\sin\theta\,\rho u_\theta) + \frac{1}{R\sin\theta}\frac{\partial \rho u_\phi}{\partial\phi} = 0.$$

2. The R-component of the momentum equation:

$$\frac{\partial u_R}{\partial t} + u_R\frac{\partial u_R}{\partial R} + \frac{u_\theta}{R}\frac{\partial u_R}{\partial\theta} + \frac{u_\phi}{R\sin\theta}\frac{\partial u_R}{\partial\phi} - \frac{u_\phi^2 + u_\theta^2}{R} = -\frac{GM}{R^2} + N_R$$

3. The θ-component of the momentum equation:

$$\frac{\partial u_\theta}{\partial t} + u_R\frac{\partial u_\theta}{\partial R} + \frac{u_\theta}{R}\frac{\partial u_\theta}{\partial\theta} + \frac{u_\phi}{R\sin\theta}\frac{\partial u_\theta}{\partial\phi} + \frac{u_R u_\theta - u_\phi^2\cot\theta}{R} = N_\theta$$

4. The ϕ-component of the momentum equation:

$$\frac{\partial u_\phi}{\partial t} + u_R\frac{\partial u_\phi}{\partial R} + \frac{u_\theta}{R}\frac{\partial u_\phi}{\partial\theta} + \frac{u_\phi}{R\sin\theta}\frac{\partial u_\phi}{\partial\phi} + \frac{u_R u_\phi + u_\phi u_\theta\cot\theta}{R} = N_\phi$$

Here the force components (including viscous force and gas pressure gradients) read:

$$\rho N_R = \frac{1}{R^2}\frac{\partial}{\partial R}\left(R^2 W_{RR}\right) + \frac{1}{\sin\theta\, R}\frac{\partial}{\partial\theta}\left(W_{R\theta}\sin\theta\right) + \frac{1}{\sin\theta\, R}\frac{\partial}{\partial\phi}W_{R\phi} - \frac{W_{\theta\theta}}{R} - \frac{W_{\phi\phi}}{R}$$

$$\rho N_\theta = \frac{1}{R^2}\frac{\partial}{\partial R}\left(R^2 W_{\theta R}\right) + \frac{1}{\sin\theta\, R}\frac{\partial}{\partial\theta}\left(W_{\theta\theta}\sin\theta\right) + \frac{1}{\sin\theta\, R}\frac{\partial}{\partial\phi}W_{\theta\phi} - \cot\theta\frac{W_{\theta\theta}}{R}$$

$$\rho N_\phi = \frac{1}{R^3}\frac{\partial}{\partial R}\left(R^3 W_{\phi R}\right) + \frac{1}{\sin\theta\, R}\frac{\partial}{\partial\theta}\left(W_{\phi\theta}\sin\theta\right) + \frac{1}{\sin\theta\, R}\frac{\partial}{\partial\phi}W_{\phi\phi}$$

Stress tensor (incl. anisotropic turbulent pressure)

$$W_{RR} = -P_g - P^t_{RR} + 2\rho\nu_t\frac{\partial u_R}{\partial R} - \frac{2}{3}\rho\nu_t \mathrm{div}\mathbf{u}$$

$$W_{\theta\theta} = -P_g - P^t_{\theta\theta} + 2\rho\nu_t\left(\frac{1}{R}\frac{\partial u_\theta}{\partial\theta} + \frac{u_R}{R}\right) - \frac{2}{3}\rho\nu_t \mathrm{div}\mathbf{u}$$

$$W_{\phi\phi} = -P_g - P^t_{\phi\phi} + 2\rho\nu_t\left(\frac{1}{R\sin\theta}\frac{\partial u_\phi}{\partial\phi} + \frac{u_R}{R} + \frac{u_\theta\cot\theta}{R}\right) - \frac{2}{3}\rho\nu_t \mathrm{div}\mathbf{u}$$

$$W_{R\theta} = \rho\nu_t\left(\frac{1}{R}\frac{\partial u_R}{\partial\theta} + \frac{\partial u_\theta}{\partial R} - \frac{u_\theta}{R}\right)$$

$$W_{\theta\phi} = \rho\nu_t\left(\frac{1}{R\sin\theta}\frac{\partial u_\theta}{\partial\phi} + \frac{1}{R}\frac{\partial u_\phi}{\partial\theta} - \frac{u_\phi\cot\theta}{R}\right)$$

$$W_{R\phi} = \rho\nu_t\left(\frac{1}{R\sin\theta}\frac{\partial u_R}{\partial\phi} + \frac{\partial u_\phi}{\partial R} - \frac{u_\phi}{R}\right)$$

axially-symmetric ($\frac{\partial}{\partial \phi} = 0$), stationary ($\frac{\partial}{\partial t} = 0$) radial accretion ($u_\theta = 0$)

Similar to sphere in viscose fluid (Landau, Lifshitz, Hydrodymamics): $u_\phi(R,\theta) = U_\phi(R)\sin\theta$

But:

1) there is a force of gravity present

2) the turbulent viscosity varies with R and can in principle depend on θ,

3) there is radial motion of matter

The ϕ-component of the momentum equation:

$$\rho\left(u_R \frac{\partial u_\phi}{\partial R} + \frac{u_R u_\phi}{R}\right) = \frac{1}{R^3}\frac{\partial}{\partial R}\left(R^3 W_{\phi R}\right) + \frac{1}{\sin\theta\, R}\frac{\partial}{\partial\theta}\left(W_{\phi\theta}\sin\theta\right)$$

angular momentum transfer by viscous forces

$$\frac{\dot{M}}{R}\frac{\partial}{\partial R}\omega R^2 = \frac{4\pi}{R}\frac{\partial}{\partial R}R^3 W_{R\phi}$$

$$\boxed{\dot{M}\omega R^2 = 4\pi R^3 W_{R\phi} + D}$$

The constant D is determined from the equation

$$D = \frac{K_1(\theta)K_2}{(1+\gamma m_t^2)} \frac{\mu^2}{R_A^3} \frac{\omega_m - \omega^*}{\omega_K(R_A)}$$

near the neutron star rotation equilibrium $\dot{\omega}^* = 0$

$$\omega_m - \omega^* = -\frac{z}{Z}\omega^* \qquad \frac{D}{|\dot{M}|} = -zR_A^2\omega^* .$$

Viscosity prescription

$$W_{R\phi} = 2\rho(-\nu_t + \nu_r)\omega + \nu_r \rho R \frac{d\omega}{dR}$$

$$\nu_r = C_1 \langle |u^t_{\parallel}| \rangle R$$

Wasiutinski (1946)

$$\nu_t = C_2 \langle |u^t_{\perp}| \rangle R$$

Angular momentum transfer equation becomes:

$$\omega R^2 \left(1 - \frac{2C_2 \langle |u^t_{\perp}| \rangle}{|u_R|}\right) = C_1 \frac{\langle |u^t_{\parallel}| \rangle}{|u_R|} \frac{Rd(\omega R^2)}{dR} - \frac{D}{|\dot{M}|}$$

General solution:

$$\boxed{\omega R^2 + \frac{D}{|\dot{M}|}\frac{1}{1-2C_2\frac{\langle|u_\perp^t|\rangle}{|u_R|}} = \left[\omega_B R_B^2 + \frac{D}{|\dot{M}|}\frac{1}{1-2C_2\frac{\langle|u_\perp^t|\rangle}{|u_R|}}\right]\left(\frac{R_B}{R}\right)^{\frac{|u_R|}{C_1\langle|u_\parallel^t|\rangle}\left(1-2C_2\frac{\langle|u_\perp^t|\rangle}{|u_R|}\right)}}$$

Near NS equilibrium rotation: $\dot{\omega}^* = 0.$ $\frac{D}{|\dot{M}|} = -z\omega^* R_A^2$, $\omega_m = (1 - z/Z)\omega^*$

1) Case of strongly anisotropic turbulence $\langle|u_\perp^t|\rangle = 0$

$$\omega_m R_A^2\left[1 + \frac{z}{1-z/Z}\left(\left(\frac{R_B}{R_A}\right)^{\frac{|u_R|}{C_1\langle|u^t|||\rangle}} - 1\right)\right] = \omega_B R_B^2\left(\frac{R_B}{R_A}\right)^{\frac{|u_R|}{C_1\langle|u^t|||\rangle}}$$

2) Anisotropy is present but $C_2\langle|u^t \perp|\rangle/|u_R|| = 1/2$,

iso-angular-momentum distribution: $\omega_m R_A^2 = \omega_B R_B^2$

3) fully isotropic: $C_2\langle|u^t \perp|\rangle/ = C_1\langle|u^t \parallel|\rangle/ = |u_R|$

$$\omega_m R_A^2 \left[1 + \frac{z}{1 - z/Z} \frac{1}{1/\epsilon - 1} \left(1 - \left(\frac{R_A}{R_B}\right)^{2-\epsilon}\right)\right] = \omega_B R_B^2 \left(\frac{R_A}{R_B}\right)^{2-\epsilon}$$

$$\epsilon = |u_R|/(C\langle u_t\rangle) \lesssim 1$$

For example, if

$\epsilon = 1/2$ near quasi-Keplerian angular rotation law can be realized.

NB: For Prandtl law

$$u_t = C_1 R^2 \left|\frac{\partial\omega}{\partial R}\right|$$

$$W_{R\phi} = \rho \nu_t R \frac{\partial\omega}{\partial R}$$

$$\nu_t = \langle u_t l_t \rangle = C_2 C_1 R^3 \left|\frac{\partial\omega}{\partial R}\right|$$

$$\rho(R) = \rho(R_A)\left(\frac{R_A}{R}\right)^{3/2}$$

$$\left|\dot{M}\right| \omega R^2 = 4\pi\rho(R_A)\left(\frac{R_A}{R}\right)^{3/2} C R^7 \left(\frac{\partial\omega}{\partial R}\right)^2 .$$

After integrating this equation, we find

$$2\omega^{1/2} = \pm\frac{4}{3}\frac{K^{1/2}}{R^{3/4}} + D_1$$

$$\boxed{\omega(R) = \frac{4}{9}\frac{|\dot{M}|}{4\pi\rho(R_A)CR_A^3}\left(\frac{R_A}{R}\right)^{3/2}}$$

So spin-up/spin-down equation for settling accretion reads

$$\boxed{I\dot{\omega}^* = Z\dot{M}\tilde{\omega}\omega_B R_B^2\left(\frac{R_A}{R_B}\right)^{2-n} - Z(1-z/Z)\dot{M}R_A^2\omega^*}$$

NB! We stress the difference in the definition of Alfven radius in this case.

$$R_A \sim \left[f(u)\frac{\mu^2}{\dot{M}\sqrt{2GM}}\right]^{2/7}, \textit{ but } f(u) \textit{ can be a function of } \mu, \dot{M}\ldots$$

3. Approximate structure of the interchange instability region

Plasma should cool down to enter magnetosphere (Elsner & Lamb 1976):

$$\mathcal{R}T_{cr} = \frac{1}{2(1+\gamma m_t^2)} \frac{\cos\chi}{\kappa R_A} \frac{\mu_m GM}{R_A}$$

Effective gravity acceleration:

$$g_{eff} = \frac{GM}{R_A^2}\left(1 - \frac{T}{T_{cr}}\right)$$

Compton cooling (Kompaneets 1956, Weymann, 1965):

$$\frac{dT}{dt} = -\frac{T - T_x}{t_C} \qquad t_C = \frac{3}{2\mu_m}\frac{\pi R_A^2 m_e c^2}{\sigma_T L_x} \approx 10.6[\mathrm{s}] R_9^2 \dot{M}_{16}^{-1}$$

$$T_{cr} \sim 30\,\mathrm{keV} \gg T_x \sim 3\ \mathrm{keV}, \qquad g_{eff} \approx \frac{GM}{R_A^2}\frac{t}{t_C}$$

the rate of instability increases with time as

$$u_i = \int g_{eff}dt = \frac{1}{2}\frac{GM}{R_A^2}t^2$$

the mean rate of the instability growth

$$< u_i >= \frac{\int u dt}{t} = \frac{1}{6}\frac{GM}{R_A^2}\frac{t^2}{t_C} = \frac{1}{6}\frac{GM}{R_A^2 t_C}\left(\frac{\zeta R_A}{< u_i >}\right)^2$$

ζR_A is the characteristic scale of the instability that grows with the rate $< u_i >$

for the mean rate of the instability growth in the linear stage we find

$$< u_i >= \left(\frac{\zeta^2 GM}{6 t_C}\right)^{1/3} = \frac{\zeta^{2/3}}{12^{1/3}}\sqrt{\frac{2GM}{R_A}}\left(\frac{t_{ff}}{t_C}\right)^{1/3} .$$

$$f(u) = \frac{< u_i >}{u_{ff}(R_A)}$$

$$f(u) \approx 0.33 \left(\frac{(\gamma - 1)(1 + \gamma m_t^2) f(\gamma, m_t)}{4\gamma\zeta} \right)^{1/33} \dot{M}_{16}^{4/11} \mu_{30}^{-1/11}$$

$$R_A \approx 0.9 \times 10^9 [\mathrm{cm}] \left(\frac{4\gamma\zeta}{(\gamma - 1)(1 + \gamma m_t^2) f(\gamma, m_t)} \frac{\mu_{30}^3}{\dot{M}_{16}} \right)^{2/11}$$

Cf. with the "canonical" expression $R_A \sim \left[\frac{\mu^2}{\dot{M}} \right]^{2/7}$

4. Spin-up/spin-down transitions (aka "torque reversals")

In the settling accretion regime: $I\dot{\omega}^* = A\dot{M}^{\frac{3+2n}{11}} - B\dot{M}^{3/11}$

$$A \approx 5.325 \times 10^{31}(0.034)^{2-n}K_1(\theta)\tilde{\omega}\delta^n \left(\frac{\zeta}{(1+(5/3)m_t^2)f(5/3,m_t)}\right)^{\frac{13-6n}{33}} \mu_{30}^{\frac{13-6n}{11}} v_8^{-2n} \left(\frac{P_b}{10\mathrm{d}}\right)^{-1}$$

$$B = 5.4 \times 10^{32}(1-z/Z)K_1(\theta) \left(\frac{\zeta}{(1+(5/3)m_t^2)f(5/3,m_t)}\right)^{\frac{13}{33}} \mu_{30}^{\frac{13}{11}} \left(\frac{P^*}{100\mathrm{s}}\right)^{-1}$$

function $\dot{\omega}^*(\dot{M})$ reaches minimum at some $\dot{M}_{cr}$

$$\dot{M}_{cr} = \left[\frac{B}{A}\frac{3}{(3+2n)}\right]^{\frac{11}{2n}}$$

$$y \equiv \frac{\dot{M}}{\dot{M}_{cr}}$$

$$\boxed{I\dot{\omega}^* = A\dot{M}_{cr}^{\frac{3+2n}{11}} y^{\frac{3+2n}{11}} \left(1 - \frac{y_0}{y^{\frac{2n}{11}}}\right)}$$

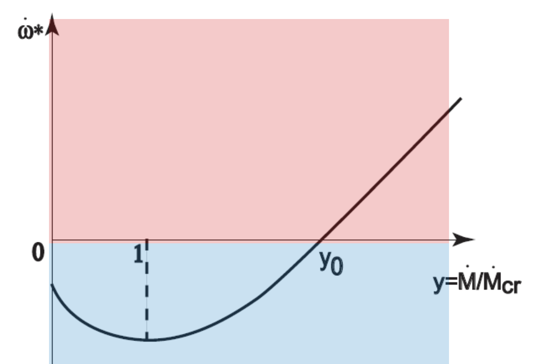

$$y_0 = \left(\frac{3+2n}{3}\right)^{\frac{11}{2n}}$$

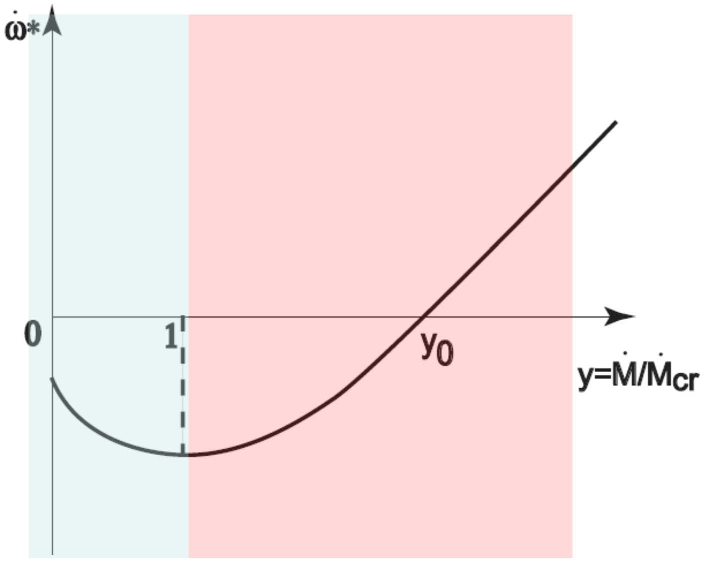

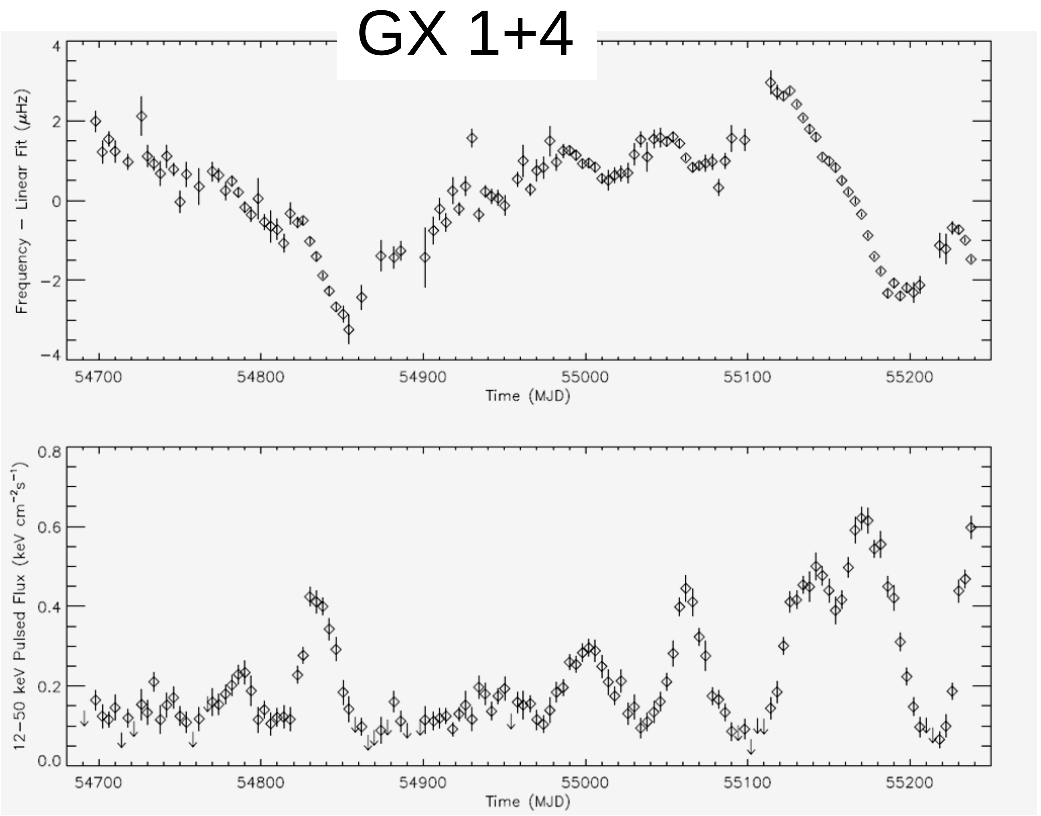

$$I(\delta\dot\omega^*) = I\frac{\partial\dot\omega^*}{\partial y}(\delta y) = \frac{3+2n}{11}A\dot M_{cr}^{\frac{3+2n}{11}}y^{-\frac{8-2n}{11}}\left(1-\frac{1}{y^{\frac{2n-1}{11}}}\right)(\delta y)\,. \qquad (52)$$

We see that depending on whether $y>1$ or $y<1$, *correlated changes* of $\delta\dot\omega^*$ with X-ray flux should have different signs. Indeed, for GX 1+4 in González-Gálan et al (2011) a positive correlation of the observed δP with $\delta\dot M$ was found using *Fermi* data. This means that there is a negative correlation between $\delta\omega^*$ and $\delta\dot M$, suggesting $y<1$ in this source.

5. Magnetic field estimate

Assuming P_* is the equilibrium NS period, we find:

$$\mu_{30}^{(eq)} \approx \left[\frac{0.0986\cdot(0.034)^{(2-n)}\tilde{\omega}}{1-z/Z}\right]^{\frac{11}{6n}} \left(\frac{P_*/100s}{P_b/10d}\right)^{\frac{11}{6n}} \left(\frac{\dot{M}_{16}(1+(5/3)m_t^2)f(5/3,m_t)}{\zeta}\right)^{\frac{1}{3}} \left(\frac{\sqrt{\delta}}{v_8}\right)^{\frac{11}{3}}$$

At the equilibrium $\dot{\omega}^* = 0$ $y = y_0$

$$A = \frac{I\left(\frac{\partial\dot{\omega}^*}{\partial y}\right)\Big|_{y_0}}{\left(\frac{3+2n}{11}\right)\frac{\dot{M}^{\frac{3+2n}{11}}}{y_0}\left(1-y_0^{\frac{-(2n-1)}{11}}\right)}$$

$\Rightarrow$ If $\left(\frac{\partial\dot{\omega}^*}{\partial y}\right)\Big|_{y_0}$ can be measured, K1, Z, etc. can be estimated

6. Application of theory to real pulsars

1. Wind-fed X-ray pulsars near equilibrium

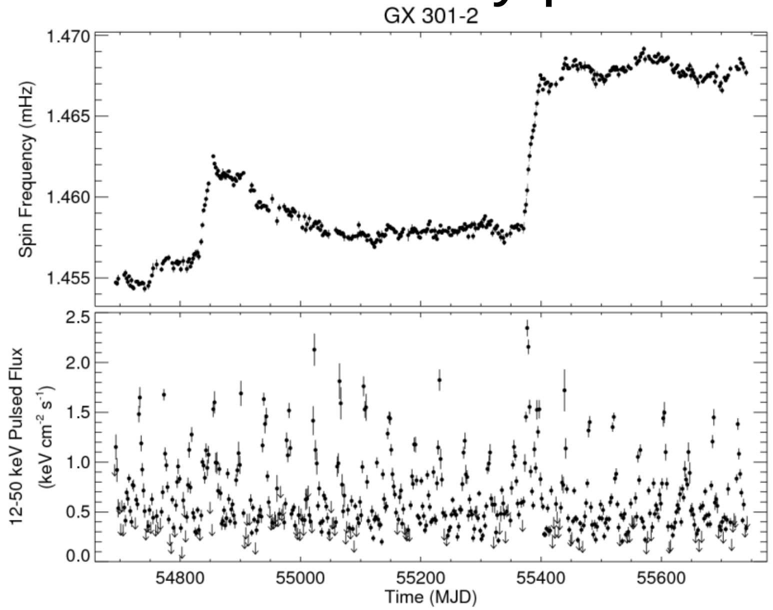

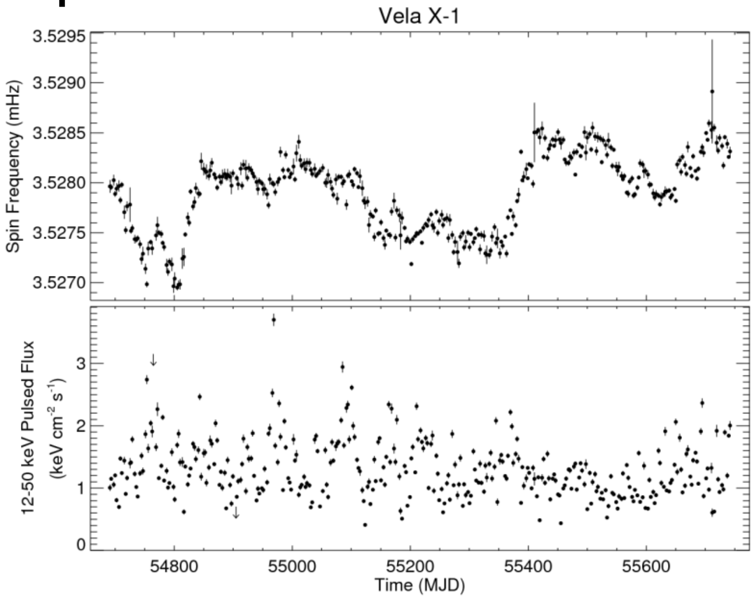

(Fermi GBM data)

2. Wind-fed pulsars with steady spin-down: GX 1+4

GX 301-2

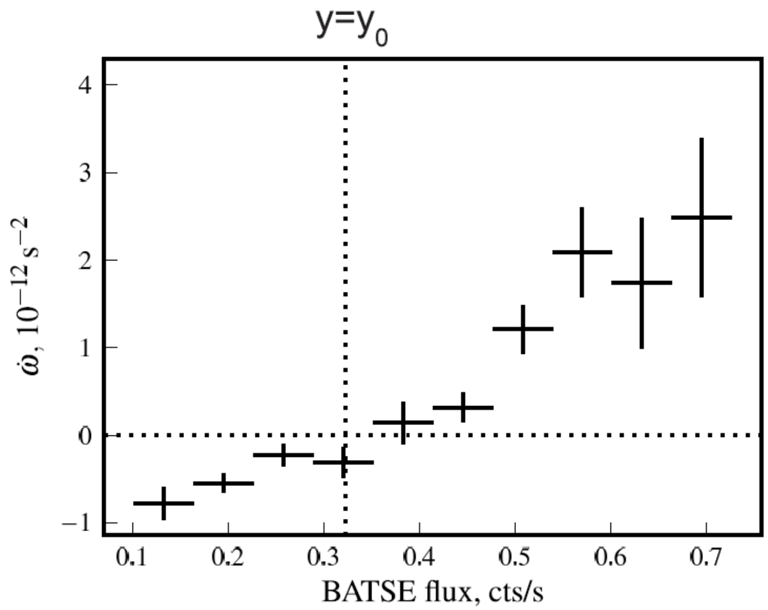

Vela X-1

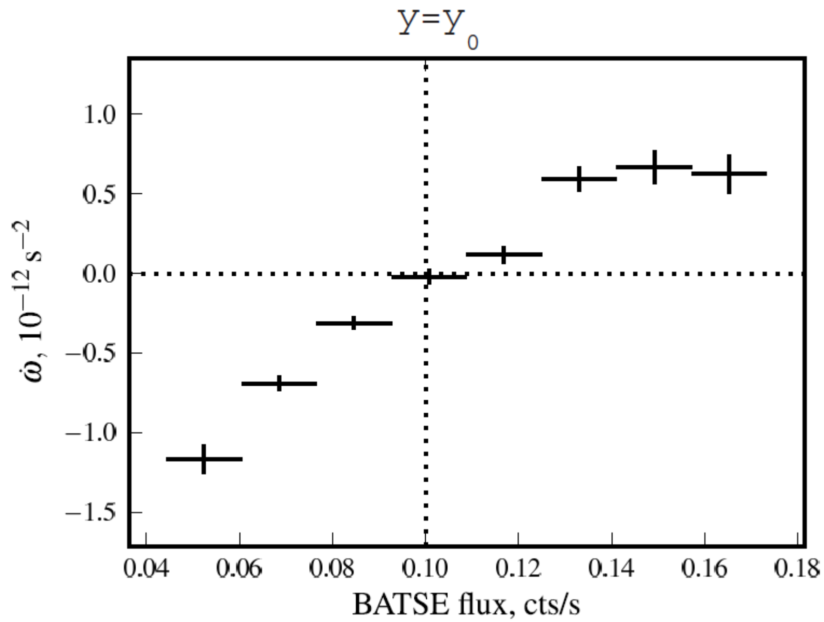

$\partial\dot{\omega}^*/\partial y \approx 4 \times 10^{-13}$ rad/s^2 $\partial\dot{\omega}^*/\partial y \approx 5.5 \times 10^{-13}$ rad/s^2

Doroshenko et al. 2010

A. González-Galán: Spin period evolution of GX 1+4

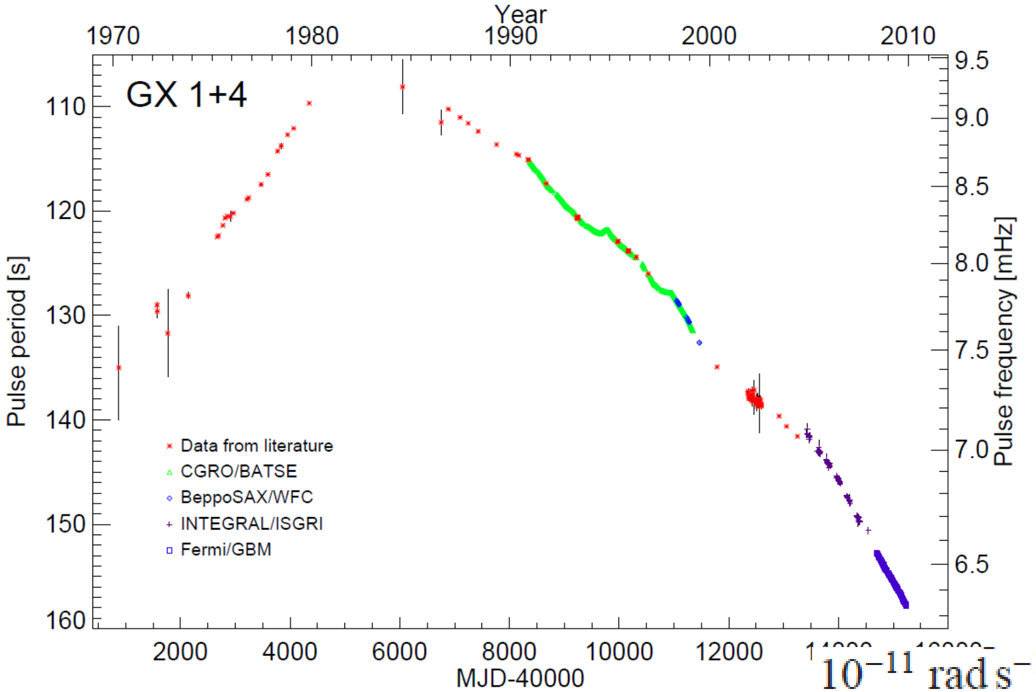

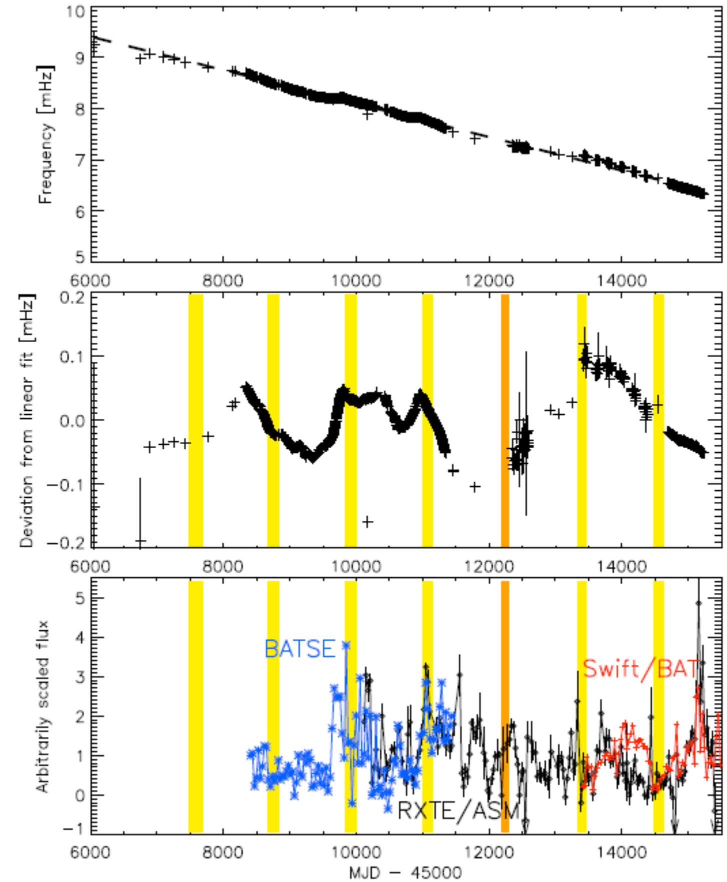

10^{-11} rad s^{-1}

$\dot{\omega}_{su} \sim 3.8 \cdot 10^{-11}$ rad/s

$\dot{\omega}_{sd} \approx -2.34\times 10^{-11}$ rad s^{-1}

Long-term spin-down variations poorly correlate (if at all) with X-ray flux variations. Most likely, due to density/velocity variations in the stellar wind

Short-term pulse frequency derivative-X-ray flux (anti)correlation (Gonzalez-Galan et al. 2010,2011)

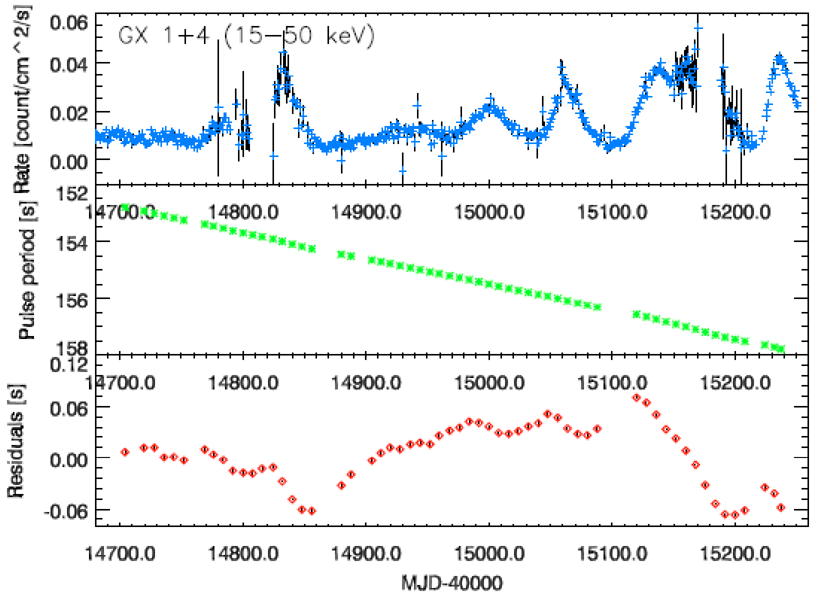

Fig. 4. *Top:* GX 1+4 Swift/BAT daily averaged light curve in the energy range 15–50 keV. *Middle:* Pulse periods derived from Fermi/GBM data. Note that the period increases from top to bottom. *Bottom:* Residuals from the pulse periods using a linear fit.

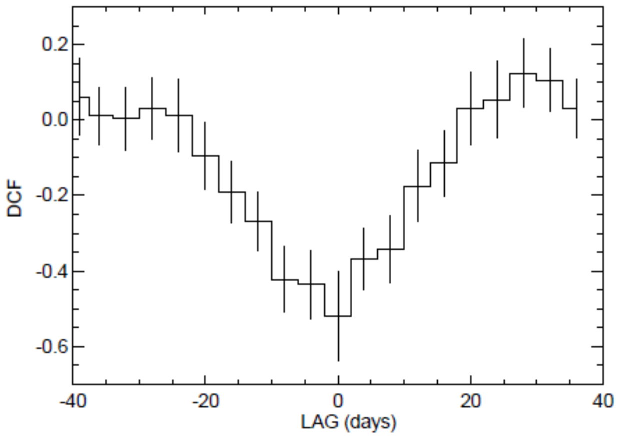

Fig. 5. The discrete correlation function (DCF), i.e., the correlation coefficient between the 15–50 keV X-ray flux and the pulse period change $\dot{\nu}$, as function of the time lag. The minimum near zero lag implies an anti-correlation between the pulse frequency derivative and X-ray flux.

$$\frac{\delta\dot{\omega}^*}{|\dot{\omega}^*|} \approx -0.2\frac{\delta\dot{M}}{\dot{M}}$$ in agreement with theory!

Pulsar	GX301 − 2		VelaX − 1		GX1 + 4	
	Measured parameters					
P_*(s)	680		283		140	
P_B(d)	41.5		8.96		1161	
v_w(km/s)	300		700		200	
$\frac{\partial\dot{\omega}}{\partial y}\|_{y_0}$	$4 \cdot 10^{-13}$		$5.5 \cdot 10^{-13}$			
$\dot{M}_{16}(\dot{\mathrm{M}}/10^{16})$	3		3		1	
	Derived parameters					
	$\mathbf{n = 2}$	$n = 3/2$	$\mathbf{n = 2}$	$n = 3/2$	$\mathbf{n = 2}$	$n = 3/2$
μ_{30}	**2.7**	0.1	**1.8**	0.16	$>$ **1.17**	> 0.02
$f(u)$	**0.42**	0.57	**0.43**	0.54		
$K_1(\Theta)$	**39**	3700	**36**	1150		
Z	**13**	910	**12**	300		
B_t/B_p	**0.1**	0.01	**0.2**	0.03		
R_A(cm)	$\mathbf{2 \cdot 10^9}$	$3 \cdot 10^8$	$\mathbf{1.6 \cdot 10^9}$	$4.2 \cdot 10^8$		
$\omega^*/\omega_K(R_A)$	**0.06**	0.004	**0.1**	0.01		

Important conclusion: unrealistic parameters for quasi-Keplerian rotation in the shell (n=3/2) suggests that almost iso-angular-momentum distribution (n=2) is realized

7. Critical X-ray luminosity

As mass accretion rate through the shell increases, so does Compton cooling; when f(u) increases up to ~0.5, the sonic point in the accretion flow locates above the Alfven surface, a free-fall gap above magnetosphere appears ➔ quasi-adiabatic shell cools down, Bondi-type accretion with NS spin-up begins

$$\dot{M}_{16}^{*} \approx 3.7 \left(\frac{\zeta}{(1 + (5/3)m_t^2) f(5/3, m_t)} \right)^{1/12} \mu_{30}^{1/4}$$

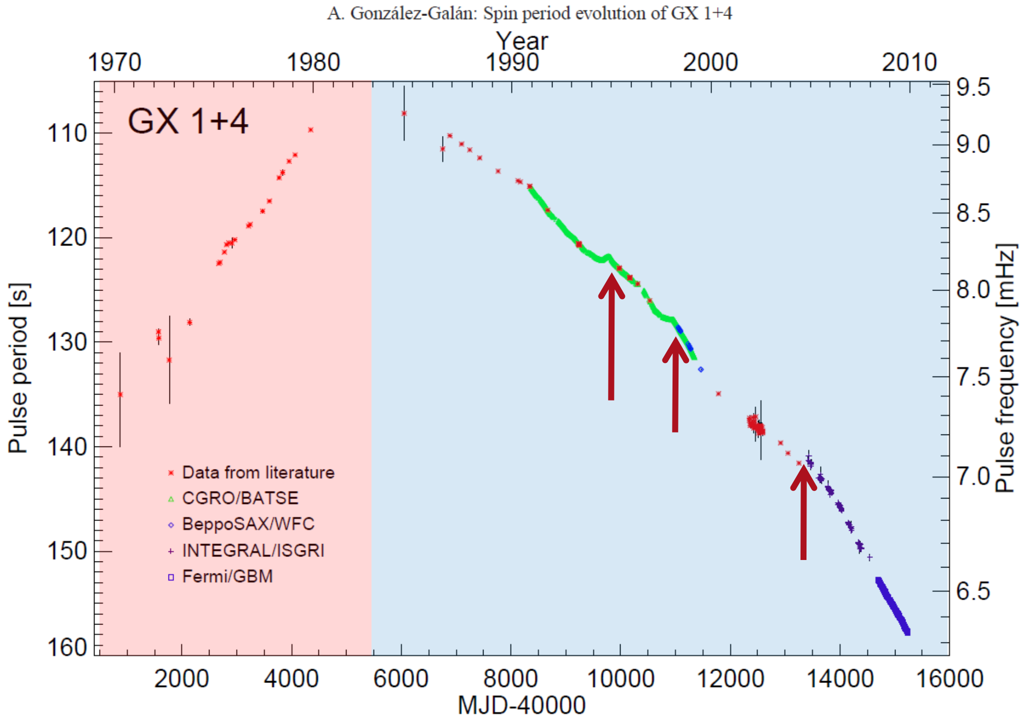

Bondi-type,
shock above
magnetosphere
no shell

Settling regime,
no shock,
convective shell

Early spin-up and short-term later spin-ups occur at X-ray luminosity 5-6 times as high as the average spin-down luminosity

8. Magnetars in HMXBs?

One should be cautious in applying formulas for disk accretion (or Alfven radius) for slowly rotating X-ray pulsars, unless firm evidence for the disk is present (usually not)

$$P_{eq,d} \approx 7\mathrm{s}\left(\frac{A_d}{B_d}\right)^{1/2} \alpha^{-1/14}\mu_{30}^{6/7}\dot{M}_{16}^{-3/7}$$

$$P_{eq} \approx 1000[\mathrm{s}]\mu_{30}^{12/11}\left(\frac{P_b}{10\mathrm{d}}\right)\left(\frac{\zeta}{(1+(5/3)m_t^2)f(5/3,m_t)\dot{M}_{16}}\right)^{4/11}\left(\frac{v_8}{\sqrt{\delta}}\right)^4\frac{(1-z/Z)}{\tilde{\omega}}$$

$\Downarrow$

P-P_B correlation on the Corbet diagram.

See poster Chashkina & Popov

Conclusions

- X-ray pulsars remain in the focus of NS studies
- Timing and spectral measurements of XPSRs allow precise measurement of orbital parameters and tiny detail of NS rotation and dynamics (e.g., disk and possibly NS precession in Her X-1 – see poster Staubert et al)
- Measurements of CRSF energy and luminosity correlations in XPSRs provide new insight into accretion columns structure
- At X-ray luminosities < 3-4 x 10^{37} erg/s wind-fed pulsars should be at the stage of subsonic settling accretion. In this regime, accretion rate onto NS is determined by the ability of plasma to enter magnetosphere.

- A gas-dynamic theory of settling accretion regime is constructed **taking into account anisotropic turbulence**. Angular momentum can be transferred through the quasi-static shell via large-scale convective motions
- Angular velocity distribution in the shell is found depending on the turbulent viscosity prescription. Comparison with observations of long-period X-ray wind-fed pulsars shows that most likely an almost iso-angular-momentum distribution is realized.
- The theory explains long-term spin-down in wind-fed accreting pulsars and properties of short-term torque-luminosity correlations.